Available online at www.sciencedirect.com
ScienceDirect
Procedia Engineering 2 (2010) 941–948
Procedia Engineering
www.elsevier.com/locate/procedia

Fatigue 2010

Crack initiation and short crack growth in metastable austenitic stainless steel in the high cycle fatigue regime

I. Roth[a,*], M. Kübbeler[b], U. Krupp[c], H.-J. Christ[a], C.-P. Fritzen[b]

[a]*Universität Siegen, Institut für Werkstofftechnik, Paul-Bonatz Str. 9-11, 57068 Siegen, Germany*
[b]*Universität Siegen, Institut für Mechanik und Reglungstechnik, Paul-Bonatz Str. 9-11, 57068 Siegen, Germany*
[c]*Fachhochschule Osnabrück, Fakultät Ingenieurwissenschaften und Informatik,Albrechtstr. 30, 49009 Osnabrück, Germany*

Received 25 February 2010; revised 11 March 2010; accepted 15 March 2010

Abstract

In the present study, the influence of the deformation-induced non-diffusional phase transformation from austenite into martensite of a metastable stainless steel on the short crack growth behaviour in the high cycle fatigue regime was investigated. For this purpose *in situ* as well as *ex situ* cyclic deformation experiments in combination with scanning electron microscopy and supplementing imaging and analytical techniques (i.e., electron backscatter diffraction for orientation and phase analysis) were employed. Cyclic loading of the AISI304L stainless steel investigated at stress amplitudes slightly above the classical fatigue limit was found to lead to a local transformation from the face centred cubic (fcc) austenite into the body centred cubic (bcc) α′-martensite. The nucleation takes place in selected areas of the microstructure in form of lamellae even already after few initial cycles near active slip systems of high Schmid factors of almost 0.5. In the majority of cases cracks initiate at twin boundaries in the absence of any martensite formation. After a first stage of shear-stress-controlled propagation along the respective twin boundary, the cracks change growth mode and direction and continue to grow in a transcrystalline manner perpendicular to the loading axis. In this stage, an alternating growth on two adjacent {111} slip systems results in low-indexed crack planes such as {100} or {110}. As a consequence of the plastic deformation at the tip of the propagating short crack a transformation into α′-martensite occurs. This martensite formation results in an increase of the specific volume and gives rise to compressive stresses leading to premature contact of the crack surfaces and hence to a retardation of the short crack growth.

Keywords: Crack initiation; short crack growth; high cycle fatigue; strain-induced transformation, metastable austenite

1. Introduction

Metastable stainless steels exhibit a diffusionless phase transformation while deep cooling or at room temperature by an additional plastic deformation [1]. The hexagonal close packed (hcp) ε-martensite and the bcc α′-martensite are formed in the fcc γ-austenite matrix [2]. The deformation-induced phase transformation has a strong influence on the fatigue behaviour. However the first nucleation of martensite occurs at a cumulative plastic strain and a plastic strain amplitude threshold must be exceeded [3]. In the regime of low cycle fatigue (LCF), the fatigue life can be

* Corresponding author. Tel.: +49-271-740-4673; fax: +49-271-740-2545.
E-mail address: Ingmar.Roth@uni-siegen.de

1877-7058
doi:10.1016/j.proeng.2010.03.102

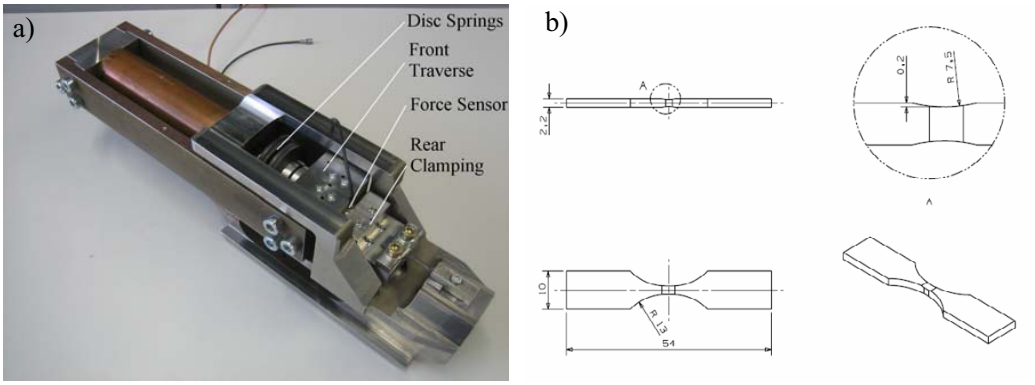

Fig. 1. (a) Miniature fatigue testing system. (b) Flat shallow notched in situ specimen.

optimised by means of a martensite formation initiated by pre-deformation [4]. For high and very high cycle fatigue (HCF and VHCF) a similar behaviour is reported. An α´-martensite volume fraction of about 26%, established by monotonic prestrain results in an optimum of the fatigue limit [5].

The transformation from the fcc lattice to the bcc lattice is accompanied by an increase of volume of 2,57% [3]. In case of fatigue crack growth of long cracks, a transformation-induced crack closure leads to a retardation of crack propagation [6, 7].

Most of the research about fatigue of metastable materials is about macroscopic characteristics such as propagation of long cracks or the correlation of martensite content with the fatigue limit. Little information about the mechanisms of crack initiation and early crack growth is available. Only Stolarz [8] reported for LCF on a high purity Fe-17Cr-13Ni stainless steel that cracks initiated exclusively in martensite regions and the propagation took place accompanied by a formation of martensite in the plastic zone of the crack tip.

The focus of this work is the determination of the microstructural mechanisms of crack initiation and short crack growth at stress amplitudes in the HCF regime and the correlation of these mechanisms to deformation-induced martensite formation. The collected data are implemented in a mechanism-based short crack model used for the simulation of short crack propagation in stainless steels. Details about this Model are reported elsewhere [9].

2. Experimental Details

2.1. Testing equipment and experimental setup

In order to observe the damage mechanisms occurring in the microstructure, two different types of testing systems for cyclic deformation were used: a newly developed piezo-driven miniature testing system (Fig. 1a) and a conventional servo-hydraulic MTS testing system.

The former system can be installed in a Phillips XL30 LaB_6 scanning electron microscope (SEM) and hence allows for *in situ* fatigue loading. It is possible to load the specimen with a maximum force amplitude of $(\Delta F/2)_{max}$=1.5 kN at a maximum frequency of f_{max}=35 Hz. With the given shallow-notch flat specimen geometry (Fig. 1b) stress amplitudes of $(\Delta\sigma/2)_{max}$=450 MPa can be obtained. During the quasi in situ experiments (intermittent the fatigue loading) micrographs in secondary electron (SE) and back scatter electron (BSE) contrast can be acquired. The local orientation of the microstructure as well as the type of phase can be determined by means of automated electron backscatter diffraction (EBSD). A detailed description of this prototype loading system is published elsewhere [10].

Using the conventional servo-hydraulic testing system, cylindrical shallow notched specimens are fatigued. For the examination of the microstructure in SEM, the specimen had to be removed periodically. All fatigue experiments

Table 1. Chemical composition of the metastable stainless steel AISI 304L (in wt. %)

	Fe	C	Cr	Ni	Si	Mn	Cu	Mo
AISI 304L	bal.	0.03	18.1	8.75	0.62	1.85	0.54	0.37

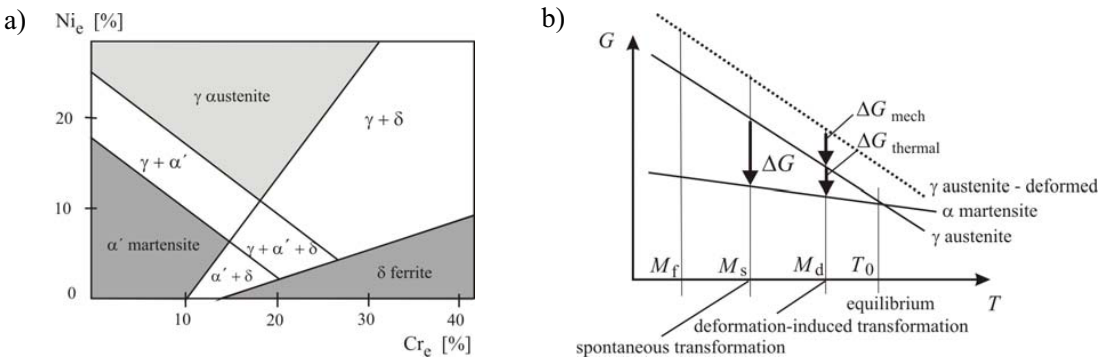

Fig. 2. (a) Phase composition of steels according to Chromium and Nickel equivalent (calculated values: Nie=10.6, Cre=19,4). (b) Schematic representation of the thermodynamic stability of austenite and α´-martensite.

are executed under fully reversed (R=–1) stress-controlled push-pull loading conditions at constant stress amplitudes close to the range of the fatigue limit ($\Delta\sigma/2$=230 MPa) of the material.

Both types of specimens were electrochemically polished prior to testing to achieve a deformation-free surface which is essential for sufficient imaging contrast and high-quality electron backscatter diffraction patterns.

2.2. Material

The material investigated in the present study was the metastable austenitic stainless steel AISI 304L (X2CrNi 18-9) delivered as cylindrical rods of 25.5 mm in diameter by the Deutsche Edelstahlwerke Suedwestfalen. The chemical composition is given in Table 1.

The material exhibited a heterogeneous microstructure with a mean grain size of approximately 15 µm and some elongated delta ferrite islands in the as-received condition. In order to homogenise the microstructure and minimise the amount of delta ferrite, the rods were annealed for 1.5 h at a temperature of 1050° C resulting in a mean grain size of 74 µm.

The phase stability of metastable austenitic stainless steels depends on the chemical composition and the temperature. The present phases after the solution annealing and cooling to room temperature can be calculated by means of the well known Schaeffler diagram [11] (Fig. 2a). From calculations using the chemical composition of the investigated material austenite and delta ferrite were predicted.

While cooling down to room temperature no spontaneous transformation will take place since the Gibbs energy difference ΔG as driving force for this process does not been reached the necessary critical value. However, this threshold value can be exceeded by an additional mechanical strain energy ΔG_{mech} as schematically shown in Fig. 2 b. In order to estimate the phase stability the M_s and the M_{d30} temperatures were calculated from phenomenological equations [12] (equation (1) and (2)) which describe the α´-martensite start temperature and the temperature where 30% plastic strain results in a 50% α´-martensite formation, respectively. Values of 72.3 °C and 40.5 °C resulted for M_s and M_{d30}, respectively.

$$M_s = 1350 - 1665(\%C+\%N) - 28(\%Si) - 33(\%Mn) - 42(\%Cr) - 61(\%Ni) \quad (1)$$

$$M_{d30} = 413 - 462(\%C+\%N) - 9.2(\%Si) - 8.1(\%Mn) - 13{,}7(\%Cr) - 20(\%Ni) - 18.5(\%Mo) \quad (2)$$

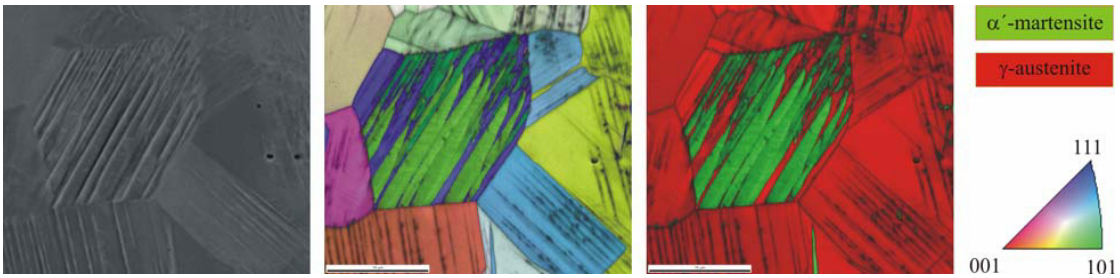

Fig. 3. α´-martensite nucleated near activated slip markings. (a) SEM micrograph; (b) EBSD inverse pole figure map (IPF); (c) EBSD phase map.

3. Experimental Results and discussion

3.1. Formation of α´- martensite under cyclic loading in the HCF regime

The cyclic loading at stress amplitudes in the regime slightly above the fatigue limit results in a comparatively low global plastic strain amplitude ($\Delta\varepsilon_{pl}/2<0.5\times10^{-4}$). However, one can recognise a high plastic activity in local areas of the microstructure. In nearly every grain, slip markings can be observed (Fig. 3). Even after the first 10^4 cycles a nucleation of α´-martensite lamellae took place in combination with activated slip systems of high Schmid factor (almost 0.5) although the global threshold for the transformation has not been exceeded [3]. From the EBSD pattern the α´-martensite formed is determined because of its bcc lattice. The inverse pole figure (IPF) map shows that the lattice orientation of the α´-martensite needles within the grains is homogeneous. Since the resolution of the EBSD technique is not sufficient for detecting very small-sized phases, no evidence for the existence of ε-martensite was observed. This phase is considered to exist only during a transition period in the transformation process from the fcc γ-austenite to the bcc α´-martensite (see e.g. [13]) and its amount is assumed to be rather low.

The crystallographic interrelationship of the parent γ-austenite and the nucleated α´-martensite lattice was derived from the EBSD orientation data. It was calculated that a closed-packed lattice plane of austenite is parallel to a closed packed lattice plane of α´-martensite. Within these planes respective closed-packed directions are parallel. This relationship is described by the *Kurdjumov-Sachs* (K-S) orientation relationship (equation (3)) [14].

$$\{111\}_\gamma \parallel \{101\}_\alpha \cap \langle 110\rangle_\gamma \parallel \langle 111\rangle_\alpha \qquad (3)$$

Due to the fact that the fcc lattice of austenite has 4 closed-packed planes and 6 closed-packed directions respectively the K–S orientation relationship leads to 24 (12 twin related) variants.

3.2. Crack initiation

It was observed that short cracks initiated near twin boundaries within a probability of approximately 70% (see Fig. 4). These cracks can be found already after 5% of fatigue life. A formation of α´-martensite before or during the crack initiation stage could not be detected.

With respect to crack initiation, the investigated metastable stainless steel seems to behave like stable austenites. It was already shown by Heinz and Neumann [15] and later again by Blochwitz and Tirschler [16] that local stress concentrations appear near twin boundaries. The high elastic anisotropy of austenitic stainless steels, which manifests itself in a high anisotropy factor of A_{304L}=3.81 (calculated according to equation 4), results in an elastic misfit that arises at the twin boundaries where the adjacent lattices are tilted by 60°. This leads to tractions on the surface and thus additional sheer stresses near the surface are produced.

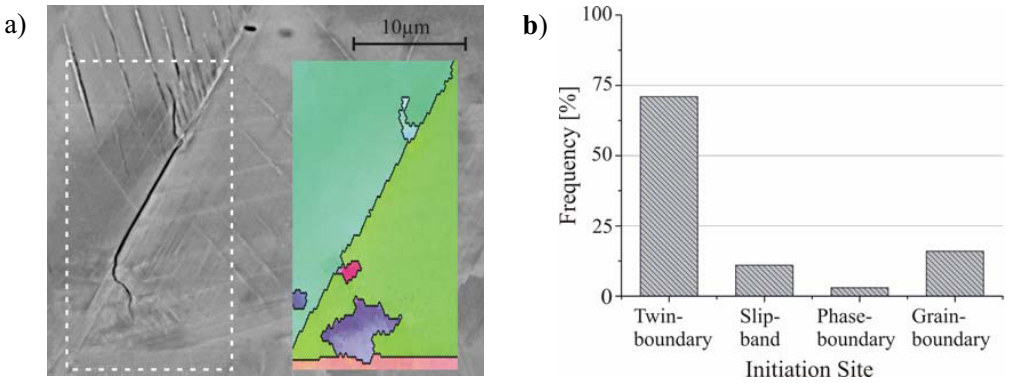

Fig. 4. Crack initiation at twin boundary. (a) SEM micrograph and inverse pole figure map (same colour code as Fig. 3); (b) statistical data about frequency of initiation site.

$$A = 2 \cdot C_{44}/(C_{11} - C_{12}),\ (C_{11}=209\ \text{GPa},\ C_{12}=133\ \text{GPa},\ C_{44}=121\ \text{GPa, data from [17]}) \quad (4)$$

Taking into account that twin boundaries in an fcc lattice structure are possible slip planes, it is obvious that cracks should initiate near these sites very likely. Heinz and Neumann introduced an "effective" Schmid-factor which combines both the fraction of the sheer stress from the applied load and the fraction of the "elastic misfit sheer stress" that arises at the twin boundary. It was shown that this effective Schmid factor could reach values of up to 1. Having determined this factor for an area containing 129 twin boundaries, they could predict the site of crack initiation near twin boundaries with high accuracy.

3.3. Short crack growth

After the crack initiation near twin boundaries, the early crack propagation takes place along the initial twin boundaries or along {111} austenite slip planes in a stage 1 of crack propagation (single slip) mode (Fig. 5). During this stage the propagation takes place without any evidence of α´-martensite formation.

In the majority of cases the cracks change their propagation direction after a few thousand cycles towards a perpendicular direction with respect to the applied load (Fig. 5a left crack path). The cracks follow traces of low

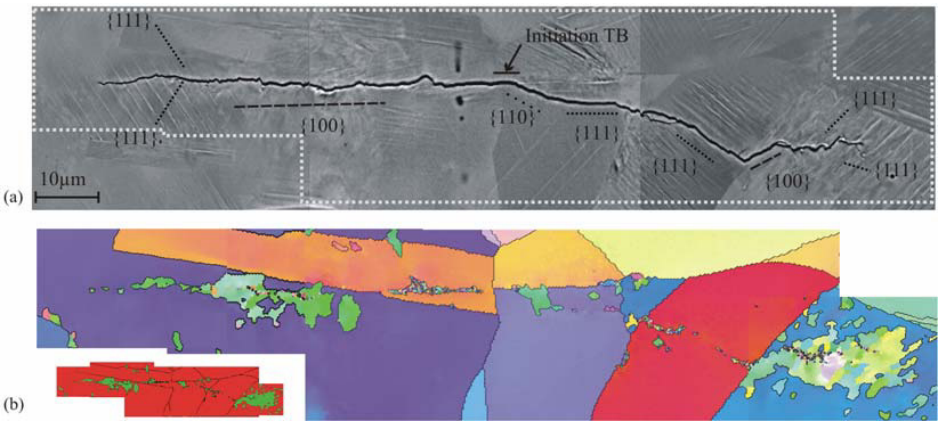

Fig. 5. Short fatigue crack. (a) SEM micrograph with indexed crack path planes; (b) EBSD inverse pole figure and phase map (for colour code see Fig. 3).

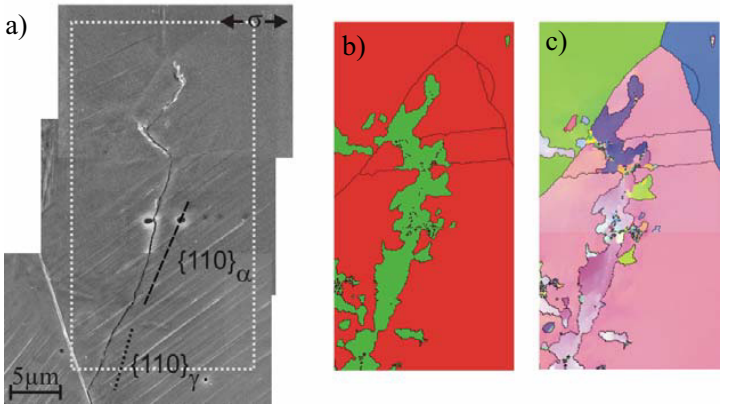

Fig. 6. Short crack path. (a) SEM micrograph with indexed crack path planes; (b) EBSD IPF map (c) EBSD phase map (for legend see Fig. 3).

indexed austenite lattice planes such as {110} or {100}. This could be a result of a kind of double-slip crack propagation with crack growth on to adjacent {111} austenite slip systems as it was described for the austenitic grains in duplex stainless steel in [18] and termed as a stage 1b crack growth. In stable stainless steel this propagation mechanism was explained as a plastic blunting/resharpening-based stage 2 crack growth [19]. While propagating in the depict manner, a nucleation of α′-martensite in the plastic zone in front of the crack tip can be observed. The formed α′-martensite appears blocky.

In the early phase of this crack propagation stage, the orientation of the α′-martensite formed is homogeneous (Fig. 6). A superposition of α′-martensite nucleation and crack growth seems to take place. This is a consequence of the described double slip or blunting/resharpening mechanism. The plastic activity ahead of the crack tip is high and a nucleation of α′-martensite takes place. Simultaneously, the crack propagates on an α′-martensite slip plane (here {110}) in a single slip mode. The assumption of pronounced α′-martensite formation in the double slip crack propagation mode is supported by α′-martensite nucleation theories. Several authors (see e.g. [20–23]) have reported that deformation-induced α′-martensite nucleates at intersection of shear bands. Different approaches of the relevant mechanisms have been published based on transmission electron microscopy investigations. All assumptions have in common that due to low stacking fault energy the movement of dislocations or partial dislocations result in bands of stacking faults, stacks of twins or the hcp ε′-martensite. At intersections of those shear bands the nucleation of α′-martensite was observed. So the formation of α′-martensite ahead of the crack tip is likely to occur when several crossing slip systems are active resulting in a high number of intersecting shear bands as it is the case in double slip mode.

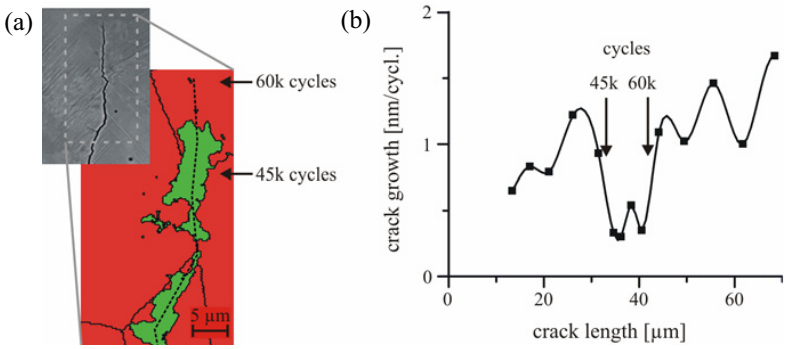

Fig. 7. Short crack closure effect. (a) EBSD phase map; (b) crack growth vs. crack length.

For some short cracks a change of the propagation direction back to a {111} austenite direction (single slip mode) was observed accompanied by a strong decrease of formation or even complete lack of transformed α′-martensite (Fig. 5a right crack path). This evidence supports the assumption of the double-slip α′-martensite nucleation mechanism superimposed with single-slip short crack growth on an α′-martensite slip system.

With increasing crack length the transformed zone becomes bigger and the orientation of the α′-martensite formed fluctuates. This explains why the crack path appears zig zag like and why an indexing of the crack path orientation is not longer possible (Fig. 5, right crack tip).

In this state a deceleration of the crack propagation can be observed as a result of the volume increase of the formed α′-martensite. While propagating through a large area of α′-martensite, which was formed in the plastic zone of the crack tip, a strong drop of crack growth rate occurs. This effect can be attributed at least to two mechanisms. Firstly, the volume expansion ahead of the crack tip should significantly reduce the tensile stress field in front of the crack. Secondly, analogue to the crack closure behaviour of long cracks [6,7], α′-martensite causes compression stresses in the wake of the propagating crack which should lead to a premature contact of the crack surfaces and thus to a transformation-induced crack closure effect.

4. Summary and Conclusion

The micro structural mechanisms of crack initiation and short crack growth in the metastable stainless steel AISI 304L under fatigue loading in the HCF regime were investigated. The results can be summarised as follows:

- While cycling at stress amplitudes near the fatigue limit, high plastic activity in local areas of the microstructure was observed. Nearly every grain showed slip markings, in some of them lamellae of α′-martensite located near activated slip systems of high Schmid factors were formed.
- The crystallographic orientation relationship between the γ-austenite matrix and the formed α′-martensite was found to fulfil as the *Kurdjumov-Sachs* relationship.
- The initiation of short cracks can be observed already after 5% of fatigue life. With a probability of about 70%, it takes place next to twin boundaries without any connection to martensite formation. Due to the high elastic anisotropy of the material, an elastic misfit arises between the twin grains which leads to an additional sheer stress on the twin boundary. As a consequence, a high slip activity takes place in or close to twin boundaries giving rise to crack initiation.
- The early crack propagation takes place along the initial twin boundary or a {111} slip plane in stage 1 single-slip crack propagation mode without any observable formation of α′-martensite. After this the crack changes its direction towards a direction perpendicular to the applied load. In this stage the crack seems to follow low indexed austenite lattice planes such as {110} or {100} accompanied by a nucleation of α′-martensite in the plastic zone in front of the crack tip. A superposition mechanism of α′-martensite nucleation and crack growth is suggested by the authors; in the zone of the crack tip the α′-martensite is formed by a double slip mode superimposed by a single slip crack growth on an α′-martensite {110} slip plane.
- Evidence for stress field reduction and/or transformation induced crack closure of short cracks is given since a retardation of crack velocity occurs while propagating through large areas of α′-martensite formed.

Acknowledgements

The financial support by the Deutsche Forschungsgemeinschaft under grant No. PAK 104 is gratefully acknowledged.

References

[1] Nishiyama Z. *Martensitic Transformation*. New York: Academic Press; 1978.

[2] Krupp U, West C, Christ HJ. Deformation-induced martensite formation during cyclic deformation of metastable austenitic steel: Influence of temperature and carbon content. *Mater Sci Eng A* 2008;**481–482**:713–17.

[3] Bayerlein M, Christ HJ, Mughrabi H. Plasticity-induced martensitic transformation during cyclic deformation of AISI304L stainless steel. *Mater Sci Eng A* 1989;**114**:L11–L16.

[4] Maier HJ, Donth B, Bayerlein M, Mughrabi H, Maier B, Kesten M. Optimierte festigkeitssteigerung eines metastabilen austenitischen stahls durch wechselverformungsinduzierte martensitumwandlung bei tiefen temperaturen. *Z Metallkd* 1993;**84**:820–6.

[5] Mueller-Bollenhagen C, Zimmermann M, Christ HJ. Very high cycle fatigue behaviour of austenitic stainless steel and the effect of strain-induced martensite. *Int J Fatigue* 2010;**32**:936–42.

[6] Hornbogen E. Martensitic transformation at a propagating crack. *Acta Metall* 1977;**26**:147–52.

[7] Mayer HR, Stanzl-Tschegg SE, Sawaki Y, Huehner M, Hornbogen E. Influence of transformation-induced crack closure on slow fatigue crack growth under variable amplitude loading. *Fatigue Fract Eng Mater Struct* 1995;**9**:935–48.

[8] Stolarz J, Baffie N, Magnin T. Fatigue short crack behaviour in metastable austenitic stainless steels with different grain sizes. *Mat Sci Eng A* 2001;**319-321**:521–6.

[9] Kübbeler M, Roth I, Krupp U, Fritzen CP, Christ HJ. Simulation of stage 1-crack growth using a hybrid boundary element technique. *Eng Fract Mech* 2010;doi:10.1016/j.engfracmech.2010.01.004.

[10] Krupp U, Roth I, Christ HJ, Kübbeler M, Fritzen CP. In-situ SEM observation and analysis of martensitic transformation during short fatigue crack propagation in metastable austenitic steel. *Adv Eng Mater* 2010;submitted.

[11] Schaeffler AL. Constitution diagram for stainless steel weld. *Metal Progr* 1949;**56**:680.

[12] Cina B. Effect of cold work on the gamma to alpha transformation in some Fe-Ni-Cr alloys. *J Iron Steel Inst* 1954;**177**:406.

[13] Fujita FE. On the lattice deformation in martensite transformation of steel. *Metall Trans A* 1977;**8A**:1727–36.

[14] Kurdjumov G, Sachs G, Über den mechanismus der stahlhärtung. *Z Phys* 1930;**64**:325–43.

[15] Heinz A, Neumann P. Crack initiation during high cycle fatigue of an austenitic steel. *Acta Metall Mater* 1990;**38**:1933–40.

[16] Blochwitz C, Tirschler W. Twin boundaries as crack nucleation sites. *Cryst Res Technol* 2005;**40**:32–41.

[17] Ledbetter HM. Predicted monocrystal elastic constants of 304 type SS. *Physica B* 1985;**128**:1–4.

[18] Dueber O, Kuenkler B, Krupp U, Christ HJ, Fritzen CP. Experimental characterization and two-dimensional simulation of short-crack propagation in an austenitic-ferritic duplex steel. *Int J Fatigue* 2006;**28**:983–92.

[19] Blochwitz C, Jacob S, Tirschler W, Grain orientation effects on the growth of short fatigue cracks in austenitic stainless steel. *Mater Sci Eng A* 2008;**496**:59–66.

[20] Olsen GB, Cohen M. Kinetics of strain induced martensitic nucleation. *Metall Trans A* 1975;**6**:791–5.

[21] Lecroisey F, Pineau A. Martensitic transformations induced by plastic deformation in the Fe-Ni-Cr-C system. *Metall Trans* 1972;**3**:387–96.

[22] Fujita H, Katayama T. In-situ observation of strain-induced gamma-epsilon-alpha prime and gamma-alpha prime martensitic transformation in Fe-Cr-Ni alloys. *Mater Trans JIM* 1992;**33**:243–52.

[23] Staudhammer KP, Murr LE, Hecker SS. Nucleation and evolution of strain-induced martensitic (bcc) embryos and substructure in stainless steel: a transmission electron microscope study. *Acta Metall* 1983;**31**:267–74.